



Tuber rugosum, a new species from northeastern North America: Slug mycophagy aides in electron microscopy of ascospores

B. Rennick, G. M. N. Benucci, Zhi-Yan Du, R. Healy & G. Bonito

To cite this article: B. Rennick, G. M. N. Benucci, Zhi-Yan Du, R. Healy & G. Bonito (2023) *Tuber rugosum*, a new species from northeastern North America: Slug mycophagy aides in electron microscopy of ascospores, *Mycologia*, 115:3, 340-356, DOI: [10.1080/00275514.2023.2184983](https://doi.org/10.1080/00275514.2023.2184983)

To link to this article: <https://doi.org/10.1080/00275514.2023.2184983>



© 2023 The Author(s). Published with license by Taylor & Francis Group, LLC.



[View supplementary material](#)



Published online: 06 Apr 2023.



[Submit your article to this journal](#)



Article views: 5092




[View related articles](#)



[View Crossmark data](#)

Tuber rugosum, a new species from northeastern North America: Slug mycophagy aides in electron microscopy of ascospores

B. Rennick ^a, G. M. N. Benucci ^a, Zhi-Yan Du ^{a,b}, R. Healy ^c, and G. Bonito ^a

^aDepartment of Plant, Soil and Microbial Science, Michigan State University, East Lansing, Michigan 48824; ^bDepartment of Molecular Biosciences and Bioengineering, University of Hawaii at Manoa, Honolulu, Hawaii 96822; ^cDepartment of Plant Pathology, University of Florida, Gainesville, Florida 32611

ABSTRACT

Species in the genus *Tuber* are ascomycetous fungi that produce hypogeous fruiting bodies commonly called truffles. These fungi are ecologically relevant owing to the ectomycorrhizal symbiosis they establish with plants. One of the most speciose lineages within *Tuber* is the Rufum clade, which is widely distributed throughout Asia, Europe, and North America and is estimated to include more than 43 species. Most species in this clade have spiny spores, and many still have not been formally described. Here, we describe *T. rugosum* based on multigene phylogenetic analysis and its unique morphological characters. *Tuber rugosum* (previously designated in literature as *Tuber* sp. 69) has been collected throughout the Midwest, USA, and Quebec, Canada, and is an ectomycorrhizal symbiont of *Quercus* trees, as confirmed through morphological and molecular analyses of root tips presented here. We also present a novel method for preparing *Tuber* ascospores for scanning electron microscope imaging that includes feeding, digestion, and spore excretion by the slug *Arion subfuscus*. Following this method, spores become free from ascus and other mycelial debris that could obscure morphological traits during their passage through the slug gut while maintaining ornamentation. Finally, we report the fatty acid analysis, a fungicolous species association, and we provide an updated taxonomic key of the Rufum clade.

ARTICLE HISTORY

Received 17 March 2022
Accepted 23 February 2023

KEYWORDS

Hypogeous fungi; phylogenetics; Rufum clade; truffles; Tuberaceae; 1 new taxon

INTRODUCTION


Although first described in 1780, truffles in the genus *Tuber* have a much longer history of being sought after due to their culinary value (Wang and Marcone 2011), which can be attributed to their unique aroma (Martin et al. 2010). The white truffle *T. magnatum* Picco and the black truffle *T. melanosporum* Vittad, for example, are amongst the most well-known and highly prized fungal species with unique aromas (Pelusio et al. 1995). Beyond their aroma, truffles are rich in carbohydrates, proteins, and unsaturated fatty acids (Bouatia et al. 2018; Yan et al. 2017), but it is still unknown how variable these traits are between *Tuber* species. In addition, the ecology and microbiology few *Tuber* species has been extensively studied (Splivallo et al. 2011), often linking fungivory by animals to the aromatic lure produced by a mature ascocarp (Hochberg et al. 2003; Maser et al. 2008).

Successful truffle spore dispersal relies on mycophagous animals detecting, consuming, and defecating mature sporocarps, as hypogeous fungi are not able to

actively discharge their spores. Numerous studies have highlighted *Tuber* spores found in animal scat, including that of pika (Cázares and Trappe 1994), northern flying squirrels (Gabel et al. 2010), crested porcupines (Ori et al. 2018), and wild boar (Piattoni et al. 2013). Passage of spores through animal digestive tracts such as the crested porcupine removes asci, may lead to some degradation of the ornamentation, and often will promote spore germination (Ori et al. 2018). Observations made while collecting specimens for this study indicated slugs, which are known to be mycophagous (Beyer and Saari 1978; McGraw et al. 2002), regularly consume truffles and other fungi that grow beneath the leaf litter of the forest floor. These observations led to the question of whether slugs could be used as an alternative to chemical preparations (e.g., Puliga et al. 2020) to obtain clean ascospores for unobstructed and improved scanning electron imaging.

Further field observations of truffles as they matured in situ led to observations of fungal infections. In 2017, Leonardi et al. reported on fungi living within eight

CONTACT B. Rennick  rennickb@msu.edu

 Supplemental data for this article can be accessed online at <https://doi.org/10.1080/00275514.2023.2184983>

© 2023 The Author(s). Published with license by Taylor & Francis Group, LLC.

This is an Open Access article distributed under the terms of the Creative Commons Attribution-NonCommercial-NoDerivatives License (<http://creativecommons.org/licenses/by-nc-nd/4.0/>), which permits non-commercial re-use, distribution, and reproduction in any medium, provided the original work is properly cited, and is not altered, transformed, or built upon in any way. The terms on which this article has been published allow the posting of the Accepted Manuscript in a repository by the author(s) or with their consent.

species of *Tuber* where they found 58.6% were infected by *Clonostachys rosea* (Link) Schroers, Samuels, Seifert & W. Gams (= *Bionectria ochroleuca* (Schwein.) Schroers & Samuels) (Leonardi et al., 2018). Other studies have indicated that yeasts including *Candida saitoana* Nakase & M. Suzuki, *Rhodotorula mucilaginosa* (A. Jörg.) F.C. Harrison, and *Trichosporon moniliiforme* E. Guého & M.T. Sm. isolated from *Tuber melanosporum* and *Tuber magnatum* ascomata produce, and may contribute to, the characteristic aroma profile of the truffles in which they are found (Buzzini et al. 2005). Mycelial fungi such as *Trichopezizella nidulus* (J.C. Schmidt & Kunze) Raitv., *Absidia cylindrospora* Hagem, and *Peniophora cinerea* (Pers.) Cooke are also known to be associated with truffle fruiting bodies (Pacioni et al. 2007). Additionally, *Aspergillus*, *Cladosporium*, *Fusarium*, *Penicillium*, and *Trichoderma* have been isolated from other truffle taxa, such as *Tuber aestivum* Vittad. and *Tuber melanosporum* ascomata (Rivera et al. 2010). Some mycoparasites are known to produce mycotoxins; thus, precautionary care should be taken to avoid consuming parasitized truffles. It has been suggested that truffles exposed on the surface of the soil are more prone to disease, although moisture levels in the environment likely play an equally important role in completing this disease triangle (Eslick 2012). In concurrence with Eslick (2012), ascomata of the species that we describe here, *T. rugosum*, sp. nov., observed with disease was subhypogeous.

The genus *Tuber* contains over 200 species, with most species diversity residing within the Rufum, Puberulum, and Maculatum clades (Bonito et al. 2010; Healy et al. 2016). Many species within these clades have yet to be formally described (Bonito et al. 2010; Healy et al. 2016). Truffles in the Rufum clade can be distinguished from those in other lineages by their smooth to slightly verrucose pale to reddish-colored peridium, stemmed ascus, and the often spiny or spinose-reticulate ornamentation of their ascospores (Healy et al. 2016). Another unique facet of the Rufum clade is the absence of cystidia on the mycorrhizal mantle they form (Healy et al. 2016). Spore ornamentation, size, shape, and dimension remain the cornerstone morphological characteristics used to describe *Tuber* species.

From 2009 through 2021, we collected truffles with morphological characteristics of those in the Rufum clade. An internal transcribed spacer (ITS) meta-analysis of *Tuber* has provided a framework by which many new species have been described (Bonito et al. 2010). Sequences of the ITS region from our specimens matched with the sequence Bonito et al. (2010) designated in the literature as *Tuber* sp. 69 (GenBank

HM485428), which we formally describe here as *Tuber rugosum*, sp. nov. In support of this new species to science, we provide (i) multigene phylogenies based on the ITS, the elongation factor 1 α (*EF1 α*), and the second-largest subunit of RNA polymerase II (*RPB2*) genes; (ii) a morphological comparison of its peridium, gleba, and spores; and (iii) a characterization of its fatty acid profile. Further, we describe an improved method for preparing spores for scanning electron microscopy (SEM) study, we identify a fungicolous species found on *T. rugosum*, sp. nov., and present a dichotomous key for the Rufum clade.

MATERIALS AND METHODS

Collection and isolation.—Truffles were collected with the aid of a hand-held four-pronged garden cultivator to remove leaf litter and explore within the upper 10 cm of forest soils. Photographs and field notes, including date, location, habitat, and fresh attributes, were made for each specimen. Specimens were stored at 4 C for a maximum of 24 h prior to morphological observations and pure culture isolation. Using forceps and sterile technique, small pieces of freshly exposed internal gleba hyphae from younger specimen were sampled and submerged into an agar medium composed of 8.0 g/L agar, 5.0 g/L potato dextrose broth, 1.5 g/L malt extract, 5.0 mL/L glycerol, and 0.82 g/L calcium nitrate. Prior to autoclaving, the pH was adjusted to 7.5 with 5.0 M sodium hydroxide. Once the postautoclave temperature fell below 50 C, 1.0 mL/L biotin (0.5 g/L stock), 1.0 mL/L chloramphenicol (60.0 mg/mL stock), and 1.0 mL/L ampicillin (50.0 mg/mL stock) were added. After initial growth on antibiotic-containing medium, a subculture was made on the same medium lacking antibiotics. These cultures were incubated at room temperature (20–22 C).

Morphological analyses.—Analysis of truffle micro-morphological characters was conducted under a compound light microscope (Leica model DM750; Buffalo Grove, Illinois). Ascospores were collected by scraping a razor blade across the gleba and mounting the fungal tissue collected on the blade on a microscope slide with 3% KOH. In total, 85 spores from 33 asci were measured and imaged at 400 \times magnification against the long and short axes, excluding ornamentation (Leica Application Suite 4.0). Length, width, and Q (length:width) measurements of the spores were then calculated, as these metrics have been informative in distinguishing species of Oregon white truffles (Bonito et al. 2010).

One immature *Tuber* sp. 69 (RH999) ascocarp used for recording developmental characters was sectioned in quarters and fixed for 2 h (4 C) in 2% glutaraldehyde + 2% paraformaldehyde in 0.1 M sodium cacodylate buffer (pH 7.2); rinsed three times in 0.1 M sodium cacodylate buffer for 20 min each; postfixed for 1 h (4 C) in 1% osmium tetroxide in 0.1 M sodium cacodylate buffer; rinsed in fresh buffer followed by three changes of deionized water for 10 min each; dehydrated in a graded ethanol series (25%, 50%, 75%, 95%, and 100%, 3× for 1 h each); infiltrated in Spurr's resin (Spurr 1969) and embedded in an aluminum dish; and polymerized for 2 days at 74 C. Sections 2 μm thick were cut with a glass knife and placed on a drop of water on a clean glass microscope slide on a warming tray. After drying, sections were stained with 0.5% toluidine blue O and preserved with a drop of per mount and a drop of xylene and a cover glass was placed on top. Images were digitally captured on a Nikon Optiphot compound microscope (Tokyo, Japan) mounted with a QImaging MicroPublisher 3.3 RTV camera (British Columbia, Canada).

Hollowed out ascocarps in close proximity to abundant slug populations of the dusky arion slug, *Arion subfuscus*, were observed. To test whether the slugs would consume truffles, we placed a single slug in a plastic container with a fresh truffle sporocarp for two sessions each lasting 4 h prior to observation. Frass contents collected from slugs that had consumed truffles were observed with a compound light microscope (Leica model DM750, Buffalo Grove, Illinois) to assess ascospore morphology. To prepare ascospores for scanning electron microscopy (SEM), slugs were maintained in a plastic box for 24 h and frass was observed after the complete *T. rugosum*, sp. nov., ascocarp had been consumed (SUPPLEMENTARY FIG. 1). The *Arion* frass was collected and visualized under a compound microscope. The ascospore-containing frass was dried at room temperature and then rinsed with phosphate-buffered saline (PBS). Ascospores not subjected to slug digestion were collected by scraping a scalpel blade across dried and rehydrated gleba and rinsed with PBS. Both sets of samples were fixed in a 4% (v/v) glutaraldehyde solution, dried with a critical point dryer (Balzers model 010; Balzers Union), and then mounted on aluminum stubs using high-vacuum carbon tabs (SPI Supplies, West Chester, PA). After the samples were coated with osmium using NEOC-AT osmium coater (Meiwafosis, Osaka, Japa), the samples were observed using a JSM-7500 F scanning electron microscope (Japan Electron Optics Laboratories (JEOL) USA, Peabody, Massachusetts).

After primary character data collection commenced, specimens were cut into sections and dried with activated silica beads. Curated holotype and paratype collections

have been deposited in the Michigan State University (MSU) Herbarium, with the MSU collection accession numbers MSC408482–MSC408486. These data have also been deposited into Mycobank MB838884.

Fungicolous species isolation.—Tissue supporting orange conidia growing from infected specimens of *T. rugosum*, sp. nov., was photographed with a Canon EOS Rebel T6 camera (Canon Inc., Tokyo, Japan) with the Laowa 24 mm f/14 2× Macro Probe lens (Venus Optics, Hefei, China) in the field prior to further processing. Photographs were taken with a shallow depth of field and were imported, aligned, and blended using Adobe Photoshop (Adobe Inc 2019b) for FIG. 3A. The fungal growth supporting the orange conidia was then placed in malt extract agar (MEA) medium composed of 10.0 g/L agar, 10.0 g/L malt extract, and 1.0 g/L yeast extract with 1.0 mL/L chloramphenicol (60.0 mg/mL stock), 1.0 mL/L streptomycin (100.0 mg/mL stock), and rifampicin (50.0 mg/mL stock). This isolate (BR428b) was incubated at room temperatures (20–22 C) and maintained on MEA with no antibiotics.

Confocal microscopy.—Confocal microscopy was performed to visualize lipid droplets within the ascocarp. Samples were sliced with a surgical scalpel and stained with 10.0 μg mL⁻¹ BODIPY 493/503 (Thermo Fisher Scientific, Pittsburgh, USA) in a phosphate-buffered saline (PBS) buffer for 2 days at 23 C. After two washes with a PBS buffer, the samples were then observed using an Olympus FV10i microscope (Olympus Scientific Solutions Americas, Waltham, Massachusetts). An argon (488 nm) laser was used for BODIPY (emission: 510–530 nm).

Lipid extraction and analysis.—Mycelium was incubated on the agar medium described above until 40.0 mm (50% colonization of Petri dish) of growth from the inoculation point was reached. The total lipid fraction was extracted from the mycelium by placing methanol-chloroform-88% formic acid (1:2:0.1 by volume) in glass tubes, followed by a wash with half volume of 1.0 M KCl and 0.2 M H₃PO₄. After phase separation by centrifugation (2000 × g for 3 min), total lipids were collected to prepare fatty acid methyl esters (FAMES) with 1.0 M methanolic HCl at 80 C for 25 min. FAMES were then extracted with hexane and analyzed by gas chromatography and flame ionization detection (Agilent, CA, USA).

Molecular analyses.—DNA was extracted from all specimens and isolated using a rapid alkaline extraction

method (Liber et al. 2022), as previously described. Ascocarp DNA was extracted by removing a small amount of the peridium and placing a 1.0-mm² piece of sterile gleba into 40.0 µL extraction solution (ES). Colonized root tips were imaged, rinsed with deionized (DI) H₂O, and placed into 20 µL ES and crushed using a pipette tip. Samples were then placed into a thermocycler set to 95 C for 10 min to lyse the cells. Following lysis, bovine serum albumin (BSA) was added at a rate of 3 times the volume of ES to help neutralize and suspend the DNA extraction. One microliter of the extracted DNA was used as template for subsequent polymerase chain reaction (PCR) amplification reactions.

Fungal rDNA was amplified with universal fungal primers ITS1F and LR3 (TABLE 1). *Tuber*-specific primers were used to amplify protein-coding genes, including the second-largest subunit of RNA polymerase II (RPB2_Tuber_f, RPB2_Tuber_r) and elongation factor 1α (EF1α_Tuber_f, EF1α_Tuber_r) (TABLE 1) following methods of Bonito et al. (2010, 2013).

Amplicon products were Sanger sequenced bidirectionally at the Research Technology Support Facility (RTSF) Genomics Core at Michigan State University on the Applied Biosystems 3730XL capillary sequencer (Waltham, Massachusetts). Sequences were trimmed with SnapGene 4.3.7 to remove low-quality regions (GSL Biotech, Chicago, Illinois). Sequences were then compared with others in the National Center for Biotechnology Information (NCBI) database with the BLASTn algorithm to verify that they were *Tuber* and to identify other entries of this taxon in the database.

Phylogenetic analyses.—Sequence alignments of taxa in the Rufum clade were made with the MUSCLE alignment algorithm (Edgar 2004) within Mesquite (Maddison and Maddison 2019). Sequence ends and highly ambiguous regions of ITS1 were excluded to eliminate ambiguous regions in the alignment. Aligned sequences were used to infer the phylogeny with maximum likelihood (ML) and Bayesian inference (BI). All ML searches were generated with Randomized Axelerated Maximum Likelihood (RAxML), and 1000 bootstrap replicates were carried out with the

GTRGAMMA nucleotide substitution model on the CIPRES Science Gateway (Miller et al. 2010; Stamatakis 2014). All BI searches were generated utilizing MrBayes on the CIPRES Science Gateway (Huelsenbeck and Ronquis 2001; Ronquist and Huelsenbeck 2003). The Markov chain Monte Carlo (MCMC) ran for 40 000 000 generations with the Metropolis-coupled Markov Chain Monte Carlo (MCMCMC) set to run four chains in parallel, sampled every 1000 cycles, and had a burn-in rate of 25% for each BI search (Geyer 1991). The model for among-site rate variation was set to INVGAMMA (inverse gamma distribution). Character sets for the ITS BI search were based on an alignment made to an annotated *Tuber brumale* Vittad. (GenBank AF106880) sequence extending from the 18S ribosomal RNA gene to the 28S ribosomal gene. The quality of the BI search was verified using MCMC files viewed with Tracer 1.7 to ensure parallel runs converge and to quantify the effective sample size (Rambaut et al. 2018). Visualization of the phylogenetic trees was performed using FigTree 1.4.4 (FigTree 2018) updated to reflect the ML bootstrap support value and BI posterior probability within Adobe Illustrator (Adobe Inc 2019a).

Dichotomous key.—A dichotomous key of described species in the Rufum clade was generated based on available species descriptions used in TABLE 3 (Butters 1903; Cao et al. 2011; Vittadini 1831; Chen et al. 2005; Deng et al. 2009; Eberhart et al. 2020; Elliott et al. 2016; Lancellotti et al. 2016; Fan et al. 2012, 2013; Frank et al. 2006; Granetti et al. 1988; Grunow and Rabenhorst 1884; Harkness 1899; Hu and Wang 2005; Leonardi et al. 2019; Suwannarach et al. 2016; Trappe et al. 1996; Uecker and Burdsall 1977; Wang 1988; Yan et al. 2018).

RESULTS

Scanning electron microscopy.—Spores that had passed through the digestive tract of the Dusky slug (*Arion* sp.) were free of nearly all of the asci remnants,

Table 1. List of primers and sequences used in this study for phylogenetic analyses.

Primer	Sequence (5' → 3')	First reported
ITS1-F	CTTGTCATTTAGAGGAAGTAA	Gardes and Bruns (1993)
LR3	CCGTGTTCAAGACGGG	Vilgalys and Hester (1990)
EF1α Tuber_f	AGCGTGAGCGTGGTATCAC	Bonito et al. (2013)
EF1α Tuber_r	GAGACGTTCTTGACGTTGAAG	Bonito et al. (2013)
RPB2 Tuber_f	YAAAYCTGACYTTRGCGTYAA	Bonito et al. (2013)
RPB2 Tuber_r	CRGTTTCCTGYTCAATCTCA	Bonito et al. (2013)

leaving relatively clean and intact ascospores for imaging. SUPPLEMENTARY FIG. 1 shows clean, ascus-free *T. rugosum*, sp. nov., spores after passage through the slug digestive tract. As seen in FIG. 5, the delicate uncinulate spines are well preserved through this digestive process, which is an improved process for obtaining high-quality SEM opportunities.

Confocal microscopy, lipid extraction and analysis.—

Confocal microscopy revealed that *Tuber rugosum*, sp. nov., BR64 and *T. floridanum* A. Grupe, Sulzbacher & M.E. Sm. contain spores that are rich in lipid droplets (green fluorescence by BODIPY staining, FIG. 4A, B). This staining made visualizing the high lipid content of the spores respective to the surrounding hyphae of the gleba evident. Further fatty acid analyses of in vitro mycelial growth showed that *T. rugosum*, sp. nov. (BR64, holotype), has about 60% of polyunsaturated fatty acids (18:2 and 18:3; FIG. 4C), whereas *T. lyonii* Butters has the highest content of unsaturated fatty acids, including 29% 18:1 (oleic acid), 34% 18:2, and 10% 20:4 (arachidonic acid) (FIG. 4D).

Molecular analyses.—*Tuber rugosum*, sp. nov., DNA sequences, including for ITS, elongation factor 1 α , and RNA polymerase II have been deposited into NCBI GenBank; see TABLE 4 for accession numbers.

Phylogenetic analyses.—The ITS (FIG. 6), elongation factor 1 α (FIG. 7A), and RNA polymerase II (FIG. 7B) phylogenetic trees all place *T. rugosum*, sp. nov., within the Rufum clade as one of the more early-divergent species. The ITS rDNA data suggest that *T. rugosum*, sp. nov., is a sister species to *T. spinoreticulatum* Uecker & Burds. with a maximum likelihood score of 91 and a Bayesian posterior probability score of 98.9 (FIG. 6). Both the elongation factor 1 α and the RNA polymerase II phylogenetic trees show the distinct placement of *Tuber rugosum*, sp. nov., near *T. spinoreticulatum* and more basal to the other taxa in the Rufum clade (FIG. 7). The elongation factor 1 α phylogenetic data provide a maximum likelihood score of 75 for the placement of *T. rugosum*, sp. nov. (FIG. 7A), and the RNA polymerase II data fall below the threshold of significance with a score of 69 (FIG. 7B).

TAXONOMY

Tuber rugosum Rennick B., Benucci G.M.N., Du Z., Healy & Bonito, sp. nov. FIG. 2
Mycobank MB838884

Diagnosis: Unique to *T. rugosum* are highly rugose zones across the peridium frequently with tight peridial folds revealing exposed gleba, characteristic echinate ascospores (mean Q = 1.1) that variably have hooked apices with an occasional subreticulate framework sloping gently away basipetally from the spines, and gene sequences.

Typification: USA. MICHIGAN: Ingham County, Onondaga township, elevation 277 m, found in soil between *Quercus rubra* and *Q. alba* in a mixed hardwood forest, 27 Aug 2018, Bryan Rennick BR64 (**holotype** MSC408483, designated here). GenBank: ITS = MW579343; *EF1a* = MW584660; *RPB2* = MW584657.

Etymology: The proposed species name references the wrinkly, or rugose, appearance of the ascocarp.

Morphology: Ascomata irregular to subglobose, irregular or lobate, 7.0–28.1 (\bar{X} = 12.7) \times 10.0–29.7 (\bar{X} = 16.8) mm diam, from opaque to translucent beige to whitish, with faint mottled gleba in mature specimen. Glebal marbling, white sterile veins and melanized yellowish beige fertile tissue. Odor mild and almost nutty; flavor mild.

Peridium 267.6 \pm 41.6 μ m thick, glabrous, large zones of rugose pellis. Pellis 139.9 \pm 7.5 μ m thick. Outermost layer 39.5 \pm 6.1 μ m thick-walled beige cells subtended by hyaline cells, isodiametric to pseudoparenchymal. Subpellis 97.3 \pm 18.9 μ m thick. In immature specimen, subpellis distinct from pellis with long, narrow, interwoven cells running perpendicular to the peridial surface. Clavate hyaline asci, 1–7 yellow-brown ascospores, most frequently with 4 ascospores. The main ovoid section of the asci 63.3–89.2 \times 28.6–62.86 μ m (\bar{X} = 75.7 \times 42.7 μ m), Q = 1.2–2.8 (\bar{X} = 1.9); peduncle from which the main ovoid section of the ascus arises 39.1–83.9 μ m (\bar{X} = 50.3 μ m) in length.

Ascospores high in lipids (FIG. 4A, B), subglobose, covered in well-spaced, uncinulate to corniform spines, having a low-sloping ridge extending away from the base and variably fusing with the ridge of adjacent spines, rarely reticulated. Ascospores in 1-spored asci are 24–32.5 \times 20.5–26.5 μ m with a shape (Q) of 1.2 and in 4-spored asci spores are 18.0–22.0 \times 16.0–20.0 μ m (Q = 1.1). Additional ascospore size and shape data are in TABLE 2. While growing in vitro, hyphae with simple septae, common branching at right angles (FIG. 1A),

Table 2. Ascospore length, width, and shape (Q) measurements based on the number of spores per asci.

Spores per asci	Spore count (n)	Length (μ m)	Width (μ m)	Q (\bar{X})
1	11	24–32.5(–37)	(19.5–)20.5–25(–26.5)	1.1–1.5 (1.2)
2	12	(19–)20.5–25(–25.5)	(17–)18.5–21.5(–22)	1.0–1.4 (1.2)
3	20	(19.5–)20–23(–24.5)	(18–)18.5–20.5(–22)	1.0–1.2 (1.1)
4	20	(16–)18–22(–23)	(15.5–)16–20(–22)	1.0–1.2 (1.1)
5	22	(18–)18.5–21.5(–22.5)	(16.5–)17–18.5(–19)	1.0–1.3 (1.1)

Table 3. Characteristics of morphologically similar *Tuber* species within the *Rufum* clade as reported in primary literature.

Species	Peridium surface	Peridium color	Peridium thickness		Pellis cell type	Pellis thickness		Subpellis cell type
			(μm)	(μm)		(μm)	(μm)	
<i>Tuber lyonii</i>	Smooth, slightly pruinose	Light chestnut brown	300–500	300–500	Interwoven	20–40	20–40	Interwoven
<i>Tuber liaotungense</i>	Verrucose	Brownish yellow	Not reported	Not reported	Pseudoparenchyma	Not reported	Not reported	Prosenchyma
<i>Tuber microspiculatum</i>	Glabrous	White yellow, pale yellow or light brown, reddish brown	200–250	200–250	Pseudoparenchyma	50–100	50–100	Interwoven
<i>Tuber quercicola</i>	Verrucose	Dark red to brownish red	250–500	250–500	Interwoven	20–100	20–100	Interwoven
<i>Tuber candidum</i>	Smooth	Light yellowish brown to reddish brown	100–300	100–300	Irregularly compact to elongated cells	30–100	30–100	Interwoven
<i>Tuber ferrugineum</i>	Papillose	Reddish	215–390	215–390	Interwoven	15–50	15–50	Interwoven
<i>Tuber nitidum</i>	Glabrous	Reddish yellow	Not reported	Not reported	Not reported	Not reported	Not reported	Not reported
<i>Tuber rufum</i>	Minutely warty to smooth	Reddish brown	Not reported	Not reported	Pseudoparenchyma	Not reported	Not reported	Interwoven
<i>Tuber melosporum</i>	Small warts	Reddish brown to reddish black	Not reported	Not reported	Pseudoparenchyma	Not reported	Not reported	Interwoven
<i>Tuber wenchuanense</i>	Smooth	Gray brown	200–250	200–250	Pseudoparenchyma	50–100	50–100	Interwoven
<i>Tuber malacodermum</i>	Smooth	Light brown	300–450	300–450	Pseudoparenchyma	Not reported	Not reported	Pseudoparenchyma to interwoven
<i>Tuber piceatum</i>	Smooth and glabrous	Pale yellow brown to yellow brown	200–350	200–350	Pseudoparenchyma	Not reported	Not reported	Interwoven
<i>Tuber crassitunicatum</i>	Smooth	Brown to yellow brown	250–300	250–300	Interwoven to pseudoparenchyma	200–250	200–250	Interwoven
<i>Tuber spinoreticulatum</i>	Leathery	Brownish gray	Not reported	Not reported	Pseudoparenchyma	150–600	150–600	Interwoven
<i>Tuber theleascom</i>	Smooth	Reddish	160–250	160–250	Pseudoparenchyma	45–150	45–150	Pseudoparenchyma to interwoven
<i>Tuber taiyuanense</i>	Smooth	Pale yellow, yellow brown or brown	150–300	150–300	Pseudoparenchyma	Not reported	Not reported	Interwoven
<i>Tuber pustulatum</i>	Low pyramidal warts	Reddish	370–550	370–550	Pseudoparenchyma	160–220	160–220	Prosenchyma
<i>Tuber lishanense</i>	Smooth	Yellow white to yellow brownish	250–350	250–350	Pseudoparenchyma	150–200	150–200	Interwoven
<i>Tuber luomaie</i>	Verrucose	Light orange brown	± 500	± 500	Subglobose or subpolyhedral	± 150	± 150	Interwoven
<i>Tuber rugosum</i>	Smooth	White to tan	267.6 ± 41.6	267.6 ± 41.6	Pseudoparenchyma	139.9 ± 7.5	139.9 ± 7.5	Interwoven
<i>Tuber umbilicatum</i>	Smooth to minute papillae	Pale yellow, yellow brown or brown	320–500	320–500	Pseudoparenchyma	90–250	90–250	Interwoven
<i>Tuber furfuraceum</i>	Smooth	Brown	340–480	340–480	Pseudoparenchyma	170–270	170–270	Interwoven
<i>Tuber huldongense</i>	Verrucose, slightly furfuraceous, pubescent	Yellow brown to red brown	150–300	150–300	Pseudoparenchyma	80–150	80–150	Interwoven
<i>Tuber lannaense</i>	Smooth	Yellow brown to dark brown	130–260	130–260	Pseudoparenchyma	35–80	35–80	Interwoven
<i>Tuber wanglangense</i>	Smooth and glabrous	Yellow white	200–250	200–250	Pseudoparenchyma	50–100	50–100	Interwoven
Species	Subpellis thickness (μm)	Average spore size (μm)	Spore shape (Q or description)	Spores per ascus	Ornamentation	Aroma	Source	
<i>Tuber lyonii</i>	Not reported	21–31 \times 17–21	Ellipsoid	1–5	Spinose to subreticulate	Pungent, nutty, malted milk	Butters (1903); Trappe et al. (1996)	
<i>Tuber liaotungense</i>	Not reported	29–40 \times 26–35	Ellipsoid	2–4	Alveolate-reticulate	Not reported	Wang (1988)	
<i>Tuber microspiculatum</i>	Not reported	22.5–35 \times 17.5–22.5	Ellipsoid	1–4	Alveolate-reticulate	Slight, not pungent	Fan et al. (2012)	
<i>Tuber quercicola</i>	130–400	20–45 \times 15–35	Ellipsoid	1–5	Curved Spines	Earthy, fresh green beans	Frank et al., (2006)	
<i>Tuber candidum</i>	70–200	19–42 \times 14–34	Globos to Ovoid	1–5	Curved Spines	Mild to slightly earthy	Harkness (1899); Frank et al., (2006)	
<i>Tuber ferrugineum</i>	200–350	28.2 \times 20.5	Ellipsoid	2–4	Spiny	Silkworm/pleasant	Carlo Vittadini (1831); Elliott et al. (2016)	
<i>Tuber nitidum</i>	Not reported	Not Reported	Ellipsoid	1–4	Echinulate	Nauseous	Carlo Vittadini (1831); Granetti et al. (1988)	

(Continued)

Table 3. (Continued).

Species	Subpellis thickness (µm)	Average spore size (µm)	Spore shape (Q or description)	Spores per ascus	Ornamentation	Aroma	Source
<i>Tuber rufum</i>	Not reported	28–42 × 18–28	Ellipsoid	4–5	Spiny	Inspid	Carlo Vittadini (1831); Grunow and Rabenhorst (1884)
<i>Tuber melosporum</i>	Not reported	40–45 × 20–25	1.7	1–6	Smooth	Garlic	Enrico et al. (2016)
<i>Tuber wenchuanense</i>	150–200	25–45 × 17.5–30	Ellipsoid	1–5	Spiny-reticulate	Not reported	Fan et al. (2013)
<i>Tuber malacodermum</i>	Not reported	26.0 ± 4.6 × 21.1 ± 3.5	1.23 ± 0.12	1–4	Spinose	Celery	Leonardi et al. (2019)
<i>Tuber piceatum</i>	Not reported	26.7 ± 2.7 × 19.2 ± 1.4	1.4 ± 0.1	1–6	Spinose	Not reported	Yan et al. (2018)
<i>Tuber crassitunicatum</i>	Not reported	29.1 ± 4.8 × 18.8 ± 2.5	1.5 ± 0.1	1–5	Spiny-reticulate	Mild	Yan et al. (2018)
<i>Tuber spinoreticulatum</i>	30–125	30–35 × 22–25	Ellipsoid	1–4	Spiny-reticulate	Rotting cabbage	Jecker and Burdsall (1977)
<i>Tuber thelascum</i>	85–120	26.6 ± 5.18 × 16.8 ± 2.63	1.59 ± 0.19	1–6	Spinose to subreticulate	Not reported	Leonardi et al. (2019)
<i>Tuber taiyuanense</i>	Not reported	20–45 × 18–30	Ellipsoid	1–5	Spiny-reticulate	Light	Cao et al. (2011)
<i>Tuber pustulatum</i>	210–350	27.4 ± 5.7 × 22.6 ± 4.55	1.22 ± 0.3	1–6	Spiny-reticulate	Acidulous to rancid	Leonardi et al. (2019)
<i>Tuber lishanense</i>	100–150	25.5 ± 3.8 × 21.6 ± 3.7	1.2 ± 0.2	1–5	Spiny	Inconspicuous	Yan et al. (2018)
<i>Tuber luomae</i>	± 350	23–30 × 18.5–23	1.21–1.32	1–5	Spiny	Mildly acrid	Eberhart et al. (2020)
<i>Tuber rugosum</i>	97.3 ± 18.9	21.5 × 19.4	1.2	1–7	Spiny	Nutty	
<i>Tuber umbilicatum</i>	150–400	23–33 × 17–23	1.4 ± 0.13	1–6	Spiny alveolate-reticulum	Not reported	Chen et al. (2005)
<i>Tuber furfuraceum</i>	170–210	25–46 × 14–27	1.7	2–5	Spiny-reticulate	Slight, not distinctive	Hu and Wang (2005)
<i>Tuber huidongense</i>	90–150	27–35 × 18–22	1.50 ± 0.18	1–5	Spiny-reticulate	Not reported	Deng et al. (2009)
<i>Tuber lannaense</i>	100–175	25–29 × 17–21	1.17 ± 0.14	1–5	Spiny-reticulate	Not reported	Suwannarach et al. (2016)
<i>Tuber wanglangense</i>	Not reported	29.9 ± 3.6 × 24.5 ± 2.6	1.2 ± 0.1	1–5	Spiny-reticulate	Not reported	Yan et al. (2018)

Note. Spore size is either based on reported average size or that of ascospores in three spore asci (Butters 1903; Cao et al. 2011; Vittadini 1831; Chen et al. 2005; Deng et al. 2009; Eberhart et al. 2020; Elliott et al. 2016; Enrico et al. 2016; Fan et al. 2012, 2013; Frank et al. 2006; Granetti et al. 1988; Grunow and Rabenhorst 1884; Harkness 1899; Hu and Wang 2005; Leonardi et al. 2019; Suwannarach et al. 2016; Trappe et al. 1996; Uecker and Burdsall 1977; Y. Wang 1988; Yan et al. 2018).

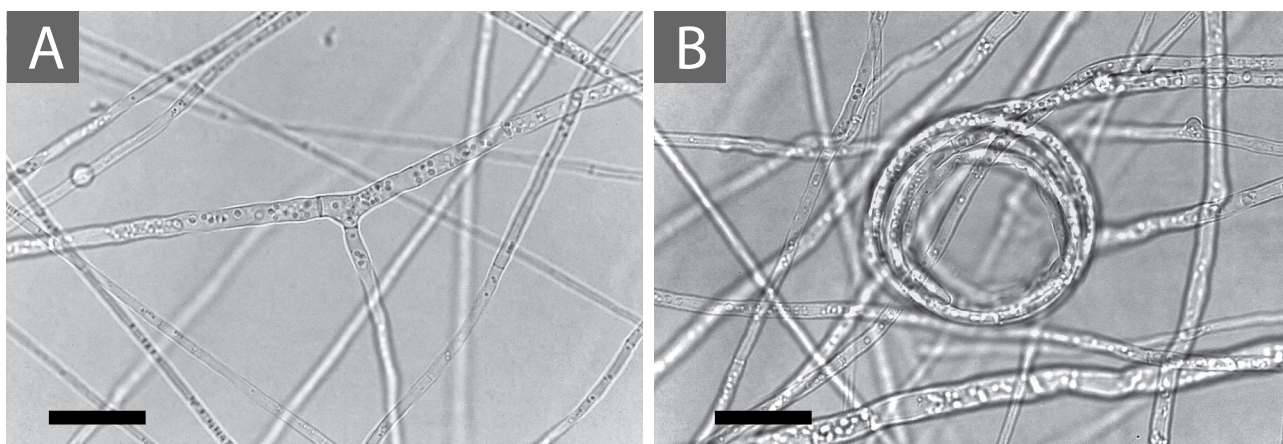


Figure 1. *Tuber rugosum* growth in vitro shown on the pH 7.0 adjusted medium containing 1.0 mL/L biotin as described in Materials and Methods. A. A typical right-angled hyphal branch with simple septa. B. A hyphal coil that is seen regularly on surface growth in cultures as they age. Bars = 20.0 μm .

rarely producing hyphal coils (FIG. 1B). Hyphae have a high content of unsaturated fats (FIG. 4B, C).

Distribution: Northeastern North America: Quebec (GenBank HM485428), Minnesota, and Michigan (see TABLE 4). The holotype of *Tuber rugosum*, sp. nov., was found within meters of an expansive collection of *T. floridanum* and *T. brennemanii* A. Grupe, Healy & M.E. Sm.

Habitat, distribution, and phenology: Northeastern North America from Michigan and Minnesota, USA, through Quebec, Canada. Collected Jul–Nov; hypogeous to subhypogeous in previously disturbed soil of mixed hardwood forest dominated by *Quercus rubra* and *Q. alba*.

Additional specimens examined: USA. MINNESOTA: Stearns County, found hypogeous in mixed conifer and deciduous forest, 17 Oct, 2009, *Rosanne Healy RH1030* (FLAS-F-61987); MICHIGAN: Ingham County, found hypogeous in mixed hardwood dominated by *Q. rubra* and *Q. alba*, 17 Jul 2017, *Bryan Rennick BR48* (MSC408482); *ibid.*, found subhypogeous in mixed hardwood dominated by *Q. rubra* and *Q. alba*, 7 Aug, 2019, *Bryan Rennick BR145* (MSC408484); *ibid.*, found hypogeous in mixed hardwood dominated by *Q. rubra* and *Q. alba*, 18 Aug 2019, *Bryan Rennick BR159* (MSC408485); *ibid.*, found subhypogeous in mixed hardwood dominated by *Q. rubra* and *Q. alba*, 11 Sep 2020, *Bryan Rennick BR378* (MSC408486); *ibid.*, found subhypogeous in mixed hardwood dominated by *Q. rubra* and *Q. alba*, 4 Sep 2021, *Bryan Rennick BR428a* (MSC409443).

Notes: Both *T. rugosum* and *T. spinoreticulatum* share a distinctive small cavity revealing gleba on most ascoma, as seen in FIG. 2A. Additionally, they share similar habitats among oak trees, found in northeastern North America, with pseudoparenchyma cells forming the pellis

and interwoven cells forming the subpellis. However, *T. rugosum* has a smooth, white to tan peridium surface, whereas *T. spinoreticulatum* has a leathery, brownish gray peridium. Their aroma also differs in that *T. rugosum* has a nutty aroma but *T. spinoreticulatum* smells of rotten cabbage (Uecker and Burdsall 1977). Finally, *T. rugosum* has small, spiny ascospores at $16.1\text{--}25.7 \times 15.4\text{--}22.0 \mu\text{m}$, but *T. spinoreticulatum* has larger spiny-reticulate ascospores at $30\text{--}35 \times 22\text{--}25 \mu\text{m}$.

On the same agar medium described in Materials and Methods, *Tuber rugosum* grows vegetatively with right-angled branching and simple septae, as shown in FIG. 1A. In older cultures (FIG. 1B), hyphal coils can be seen once the culture becomes stressed.

We found some collections of *T. rugosum* that were infected by a fungicolous species that we identified as *Clonostachys rosea*. When infected by *C. rosea*, the aroma was particularly smoky and the peridium turned a darker shade with more pronounced red-brown hues, as shown in FIG. 3. The *Clonostachys rosea* isolate (BR428b) maintained a faint smoky aroma from the pure isolate after more than two transfers beyond the initial isolation plate, but directed experiments will be needed to test the impact of this mycoparasite on truffle aroma. Cultures of the holotype (BR64) as well as *C. rosea* (BR428b) are available upon request.

DISCUSSION

Here, we described a new truffle species, *T. rugosum*, as supported by three independent phylogenetic markers, as well as by morphological characters. Phylogenetic reconstructions demonstrate this species as a novel North American species in the Rufum clade. *Tuber*

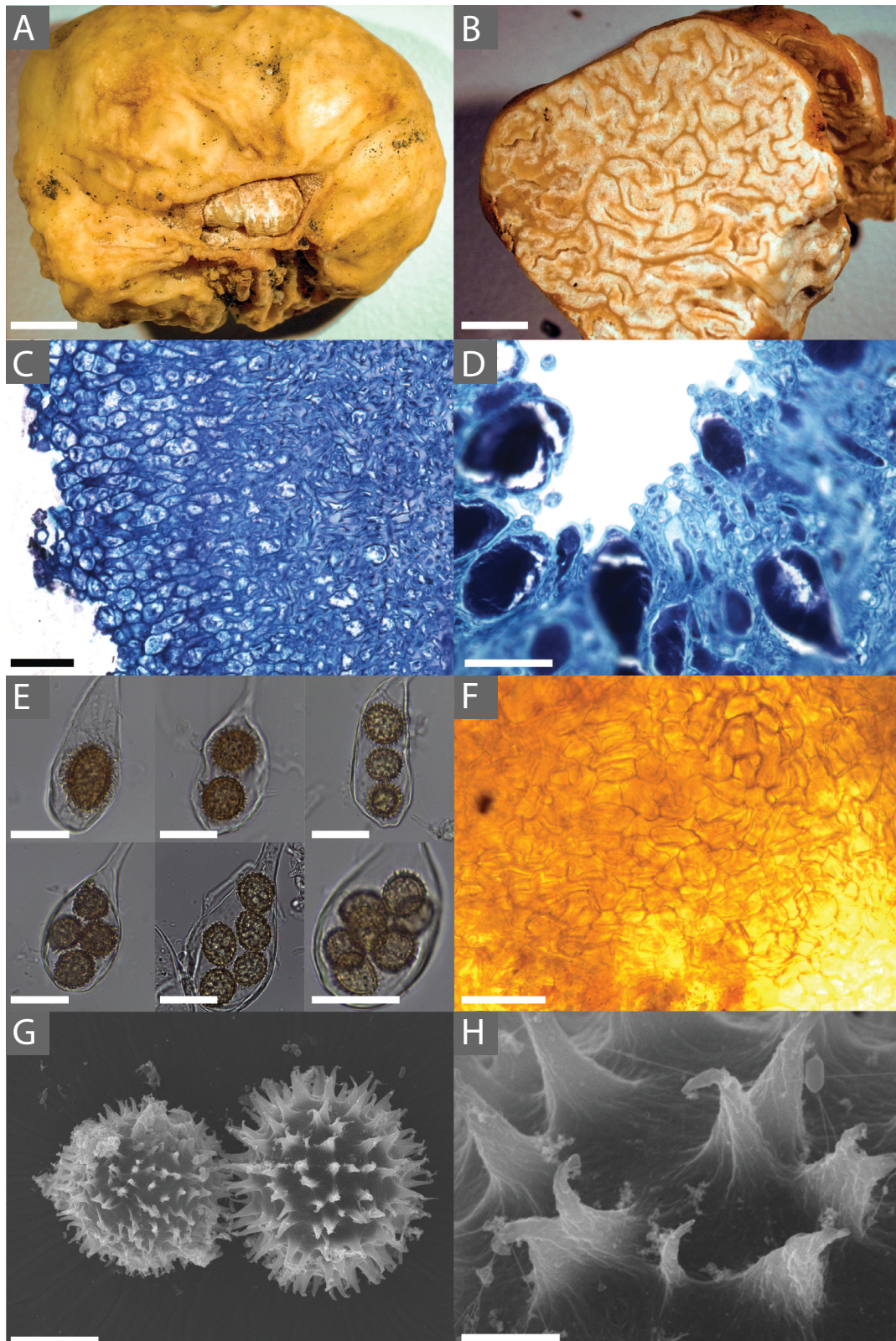
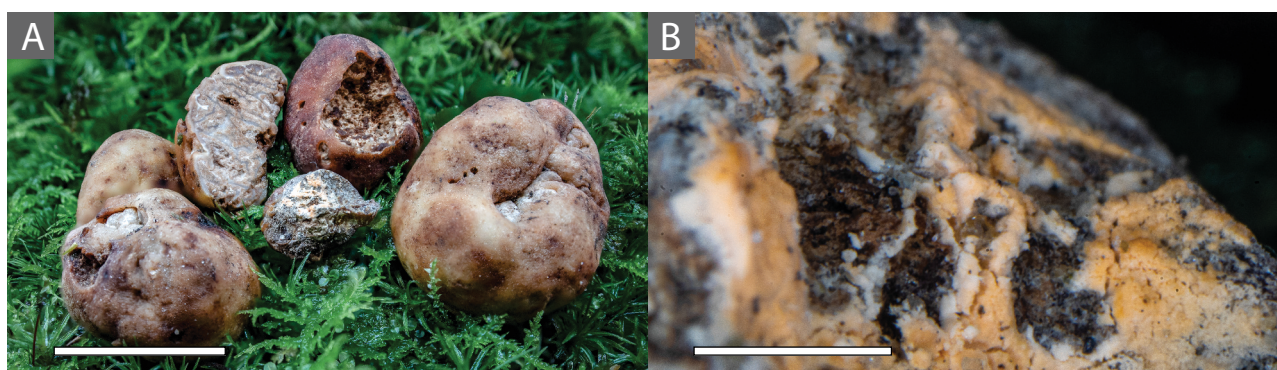


Figure 2. A. *Tuber rugosum* (BR64, holotype) ascocarp showing both the rugose peridium and exposed sterile gleba. B. A cross-section of *T. rugosum* (BR64) showing the gleba and its marbling. C. A cross-section (stained with toluidine blue O) of *T. rugosum* (RH999) showing the distinctive long, narrow cells of the immature peridium. D. Hymenium (stained with toluidine blue O) of an immature specimen showing the developing asci and paraphyses. E. Ascii of *T. rugosum* (BR64) containing 1, 2, 3, 4, 5, and 7 ascospores. F. Mantle of *T. rugosum* (GenBank MW579340) on the root tip of a red oak (*Quercus rubra*). G. SEM image of a *T. rugosum* ascospore (BR64) showing the echinate surface. H. SEM image showing details of the uncinulate spines on the ascospore of *T. rugosum* (BR64, holotype; GenBank MW579336). Bars: A, B = 6.0 mm; C, F = 50.0 μ m; D = 25.0 μ m; E = 30.0 μ m; G = 10.0 μ m; H = 2.0 μ m.

Table 4. *Tuber rugosum* collections used in this study with their herbarium and GenBank accession numbers and collection dates.

Species	Collection	Source	Locale	Date collected	Herbarium	Accession numbers		
						ITS	EF1a	RPB2
<i>Tuber rugosum</i>	RH999	Ascoma	USA: Minnesota	8 Aug 2009		MW584702		
<i>Tuber rugosum</i>	RH1030	Ascoma	USA: Minnesota	17 Oct 2009	FLAS-F-61987	MW584701		
<i>Tuber rugosum</i>	RH1330	Ascoma	USA: Minnesota	3 Sep 2011		MW584700		
<i>Tuber rugosum</i>	BR48	Ascoma	USA: Michigan	17 Jul 2017	MSC408482	MW579335		
<i>Tuber rugosum</i>	BR64	Ascoma	USA: Michigan	27 Aug 2018	MSC408483	MW579343	MW584660	MW584657
<i>Tuber rugosum</i>	BR145	Ascoma	USA: Michigan	7 Aug 2019	MSC408484	MW579344	MW584661	MW584658
<i>Tuber rugosum</i>	BR159	Ascoma	USA: Michigan	18 Aug 2019	MSC408485	MW579345	MW584662	MW584659
<i>Tuber rugosum</i>	BR339	Root tip	USA: Michigan	5 Aug 2020		MW579346		
<i>Tuber rugosum</i>	BR340	Root tip	USA: Michigan	5 Aug 2020		MW579347		
<i>Tuber rugosum</i>	BR342	Root tip	USA: Michigan	5 Aug 2020		MW579348		
<i>Tuber rugosum</i>	BR343	Root tip	USA: Michigan	5 Aug 2020		MW579349		
<i>Tuber rugosum</i>	BR378	Ascoma	USA: Michigan	11 Sep 2020	MSC408486	MW579975		
<i>Tuber rugosum</i>	BR428a	Ascoma	USA: Michigan	4 Sep 2021	MSC409443	OL438889		
<i>Clonostachys rosea</i>	BR428b	Anamorph	USA: Michigan	4 Sep 2021	MSC409443	OL438890		

**Figure 3.** *Tuber rugosum* ascocarp found in 2021 infected with *Clonostachys rosea*. A. The centermost ascocarp showing the darker red-brown peridium seen when infected by *C. rosea* compared with the peridium color of noninfected ascocarps. B. Orange conidia from *C. rosea* growing from the gleba of a *T. rugosum* ascocarp. Bars: A = 20.0 mm; B = 2.0 mm.

rugosum is most closely related to the North American species *T. spinoreticulatum*, and as seen in TABLE 3, the two species differ macroscopically in the color and texture of their peridium and microscopically by the size, shape, and ornamentation of their ascospores. The two species also have a different aroma, with *Tuber spinoreticulatum* being particularly unpleasant and originally described as smelling like rotten cabbage (Uecker and Burdsall 1977).

Animals play an important role in the spore dispersal of hypogeous fungi. This has been well documented in the case of small mammals, which consume truffles as food (Cázares and Trappe 1994; Gabel et al. 2010). Other animals including Diptera and Stylommatophora have fungivorous members that have been shown to enhance mycorrhizal spore dispersal, including that of truffles (Kitabayashi and Tuno 2018; McGraw et al. 2002). As documented previously, slugs in the genus *Arion* are mycophagous (Beyer and Saari 1978); however, their role in spore dispersal has not been investigated. Although this paper did not set out to determine truffle

spore viability in slug excreta, we did demonstrate that *T. rugosum* is consumed by *Arion* slugs and that spores that pass through the slug digestive tract are released from the asci in good condition for visualization. In fact, we found this to be a useful pretreatment for cleansing spores prior to preparation for SEM. Recent work by Ori et al. (2021) demonstrated that slug digestion of *T. aestivum* ascospores exhibit an altered episporial texture and increased mycorrhization of *Quercus robur* roots compared with those ascospores consumed by mice or uningested spores. Our observations that *T. rugosum* is found just beneath leaf litter and is often partially consumed raise questions on the role of *Arion* slugs and other gastropods in truffle spore dispersal in nature.

Truffles damaged by small animals or other mechanical means may also become more susceptible to infection by fungicolous organisms, which may alter its aromatic profile (Eslick 2012). It is still unknown whether *C. rosea* is a primary pathogen of truffles, although the literature suggests that *C. rosea* can be a mycoparasite of many fungal species and thus may

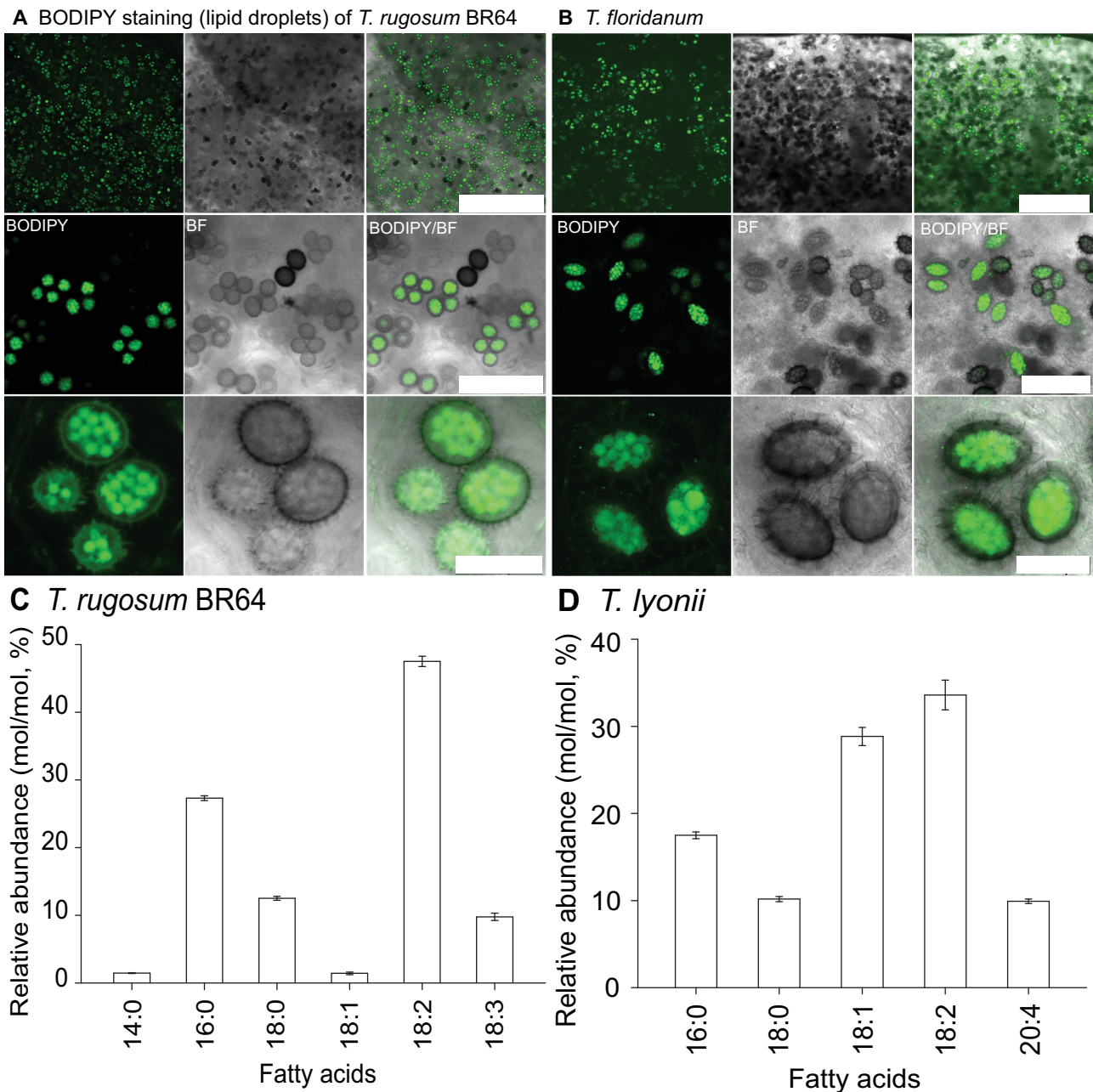


Figure 4. Lipid analysis of truffle spores. A, B. Confocal microscopy of BODIPY-stained (A) *Tuber rugosum* (BR64) and (B) *Tuber floridanum* ascospores revealing lipid content as green. C, D. FAME analysis of (C) *T. rugosum* and (D) *T. lyonii* in vitro mycelial growth showing distinct variation in fatty acid concentrations. Bars: A = 0.5 mm, 100.0 μ m, 25.0 μ m, top to bottom; B = 0.5 mm, 100.0 μ m, and 30.0 μ m, top to bottom.

have potential use as a biocontrol against fungal crop pathogens such as *Fusarium graminearum* Schwabe (Gimeno et al. 2021). In a prior report, *C. rosea* was isolated from *Tuber magnatum* but was not found to be chitinolytic (Pavic et al. 2013). We were unable to demonstrate *C. rosea* pathogenicity on *T. rugosum*, as our in vitro assays were inconclusive. While growing *C. rosea* on agar, we noted that it maintained a faint smoky aroma, which supports the hypothesis that it

contributed to the odor profile of the ascocarps it was found growing on. Other truffle-inhabiting organisms, particularly α - and β -proteobacteria, have been found to be principal contributors to sulfur-containing volatiles characteristic of *T. borchii* Vittad. ascocarp aroma (Splivallo et al. 2011). Further work is needed to ascertain the involvement of other fungi and bacteria in the aroma development and profiles of *Tuber* ascoma, as well as truffle development and disease.

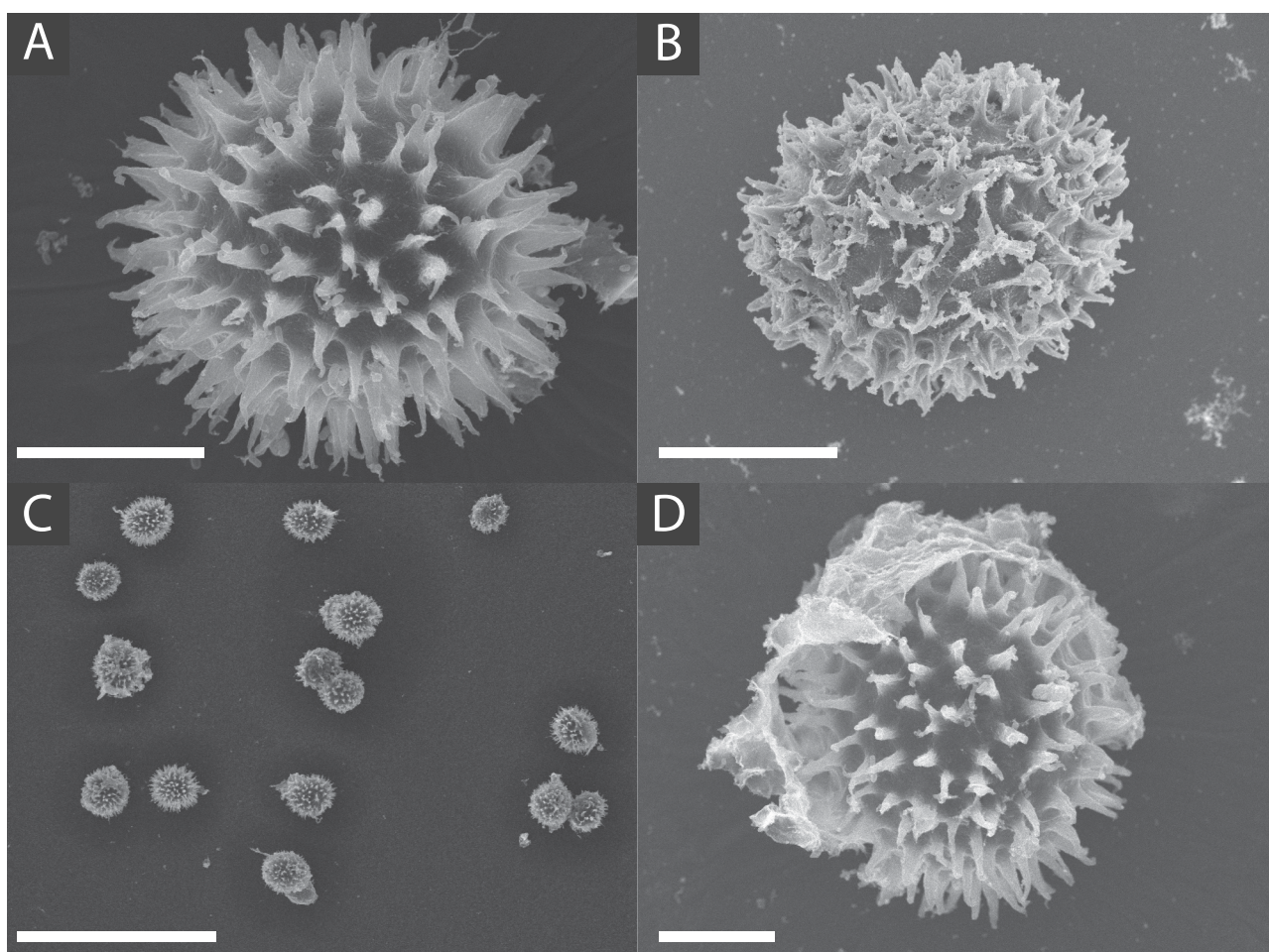


Figure 5. A. SEM image of *Tuber rugosum* ascospore having been passed through the digestive system of the dusky arion slug. B. SEM image of *T. rugosum* ascospore cleared from ascus by drying down ascocarp and scraping gleba. C. Representative cluster of *T. rugosum* ascospores subjected to the slug digestive system. D. Example of remaining ascus, digestive remnants, or other unknown tissue observed on a few of the *T. rugosum* ascospores SEM-imaged after slug digestion. Bars: A, B, D = 10.0 μm ; C = 100.0 μm .

Fatty acid profiles have been used when trying to distinguish *Tuber* species within species complexes and provide some insight into their physiology and nutrition (Angelini et al. 2015). However, *Tuber* fatty acid profiles may vary across geographic regions and under different environmental and growth conditions (Shah et al. 2020). To attempt to control for these environmental variances, we obtained pure culture isolates of *T. rugosum* and the closely related species *T. lyonii* (FIG. 4), to assess and compare FAME profiles from similarly aged mycelium grown in the same medium and environment. Truffle species had distinct fatty acid profiles from one another, with *T. rugosum* being particularly reduced in 18:1 (oleic acid) and *T. lyonii* enriched in 20:4 (arachidonic acid). Fatty acid profiles are not available for most *Tuber* species, but they could provide insights into variation in *Tuber* physiology and nutrition.

Similar to previously published ITS phylogenies (Bonito et al. 2010), *T. rugosum* is found on an early-divergent branch of the Rufum clade and appears to be sister to *T. spinoreticulatum* (FIG. 6). Our ITS ML- and BI-based phylogenies also conform to more recently published *Tuber* phylogenies (Yan et al. 2018), which placed *T. lishanense* L. Fan & X.Y. Yan and *T. piceatum* L. Fan, X.Y. Yan & M.S. Song basal to *T. spinoreticulatum* within the Rufum clade. The general structure of the phylogenetic trees analyzed from the two protein-encoding loci (FIG. 7) also agree with earlier studies (Bonito et al. 2013) but with stronger support for *T. rugosum* within the Rufum clade and its close relationship to *T. spinoreticulatum*. However, it should be noted that there are relatively few sequences available within the Rufum clade for both the *RPB2* and *EF1 α* protein-encoding regions. The lack of species representation within these protein-encoding regions is such that

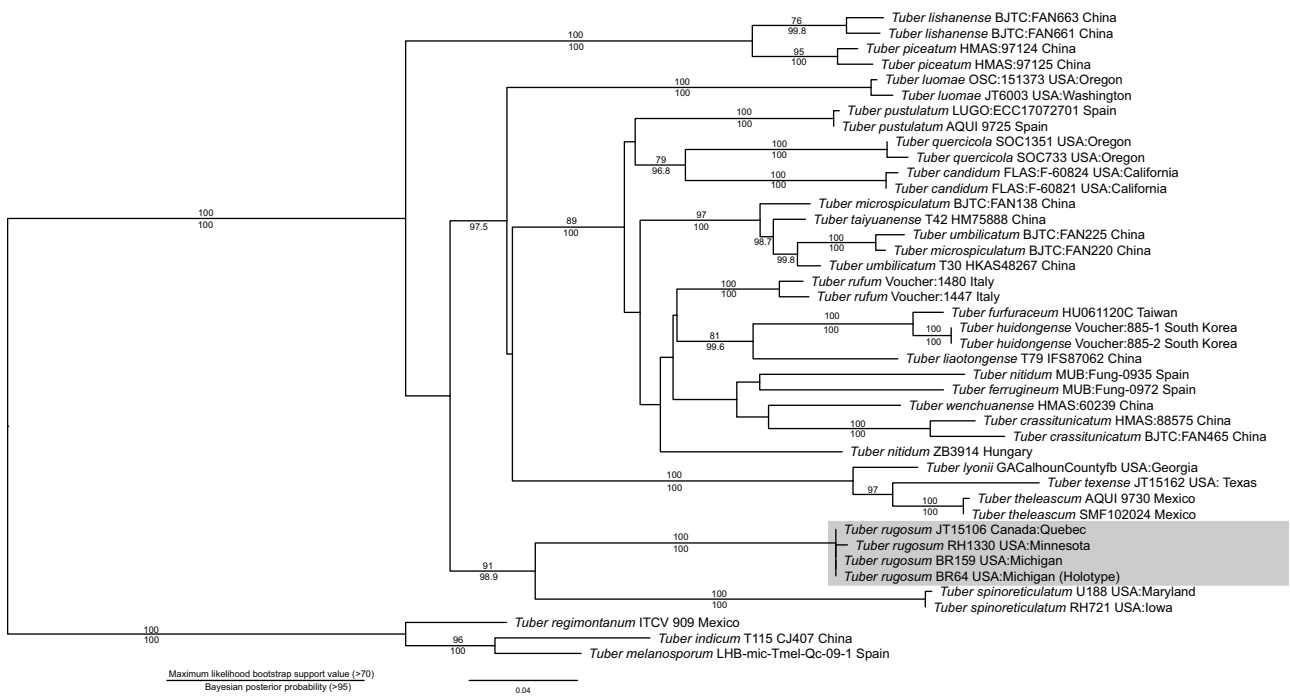


Figure 6. ITS rDNA phylogeny of the Rufum Clade. This most likely phylogenetic tree reconstructed from ITS rDNA data shows that *T. rugosum* is basal in the Rufum clade and supported as sister species to *T. spinoreticulatum*. Maximum likelihood bootstrap support values over 70 are shown above the nodes, whereas Bayesian posterior probabilities above 95 are shown below nodes. *Tuber regimontanum*, *T. indicum*, and *T. melanosporum* were included as outgroups as identified by Bonito et al. (2010). Taxa are shown with specimen, isolate, or collection number as listed in the NCBI database.

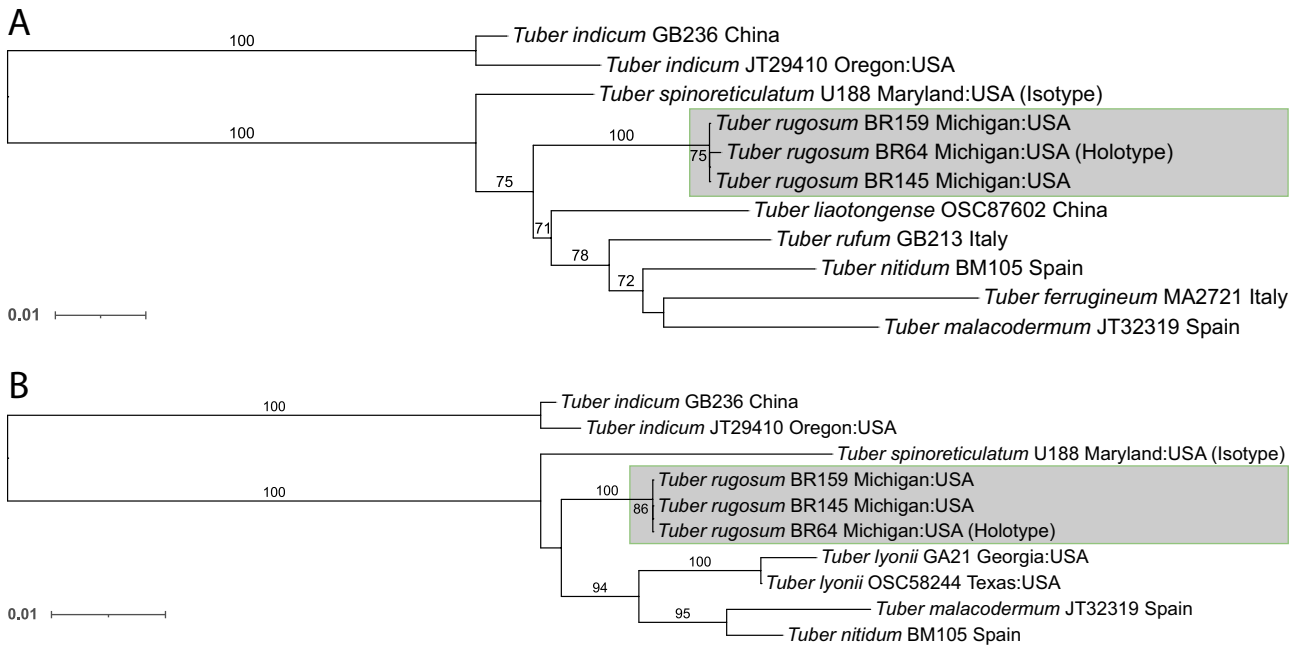


Figure 7. Elongation factor 1α (A) and RNA polymerase II gene (B) phylogenetic trees. Both show maximum likelihood bootstrap support values over 70. *Tuber indicum* was chosen as an outgroup as identified by Bonito et al. (2010). Taxa are shown with specimen, isolate, or collection number as listed in the NCBI database.

concatenating and condensing the phylogenetic trees into a single, better-supported phylogram is not possible at this time. Further work is needed to generate these protein-encoding sequences in other Rufum clade species in order to reconstruct a more comprehensive phylogeny.

In conclusion, we have described *Tuber rugosum*, a pale, wrinkly, spiny-spored truffle endemic to northeastern North America, supported by morphological and phylogenetic analyses of multiple loci. We provide the fatty acid profile of this species, describe a fungicolous species association, and present a method that involves the use of slugs to assist in cleaning ascospores prior to SEM imaging. Finally, a dichotomous key for truffles in the Rufum clade is provided below. Together, these results expand on the knowledge base of *Tuber* biodiversity and microbiome diversity in North America.

A KEY TO *TUBER* SPP. IN THE RUFUM CLADE

- | | |
|---|--|
| 1. Ascospore smooth with no ornamentation..... | 10. Found west of the Rocky Mountains |
| <i>T. melosporum</i> | <i>T. candidum</i> |
| 1'. Ascospore with ornamentation | 10'. Found east of the Rocky Mountains |
| 2 | <i>T. rugosum</i> |
| 2. European species | 11. Pellis 20–40 µm thick |
| 3 | <i>T. lyonii</i> |
| 2'. Not European species | 11'. Pellis 45–150 µm thick |
| 7 | <i>T. theleascum</i> |
| 3. Peridium smooth | 12. Outer pellis of pseudoparenchyma or globos cells ... |
| 4 | 13 |
| 3'. Peridium not smooth | 12'. Outer pellis of longer Interwoven cells |
| 5 | <i>T. quercicola</i> |
| 4. Peridium color reddish yellow | 13. Ascospore globose in shape |
| <i>T. nitidum</i> | <i>T. luomae</i> |
| 4'. Peridium color light brown | 13'. Ascospore ellipsoid in shape |
| <i>T. malacodermum</i> | <i>T. spinoreticulatum</i> |
| 5. Ascospore globose in shape | 14. Peridium verrucose or with small papillae |
| <i>T. pustulatum</i> | 15 |
| 5'. Ascospore ellipsoid in shape | 14'. Peridium smooth |
| 6 | 17 |
| 6. Pellis cells pseudoparenchyma | 15. Ascospore reticulated but with distinct curved |
| <i>T. rufum</i> | spines |
| 6'. Pellis cells interwoven | <i>T. umbilicatum</i> |
| <i>T. ferrugineum</i> | 15'. Ascospore not as above |
| 7. North American species | 16 |
| 8 | 16. Ascospore alveolate-reticulate |
| 7'. Asian species | <i>T. liaotongense</i> |
| 14 | 16'. Ascospore spiny-reticulate |
| 8. Peridium smooth | <i>T. huidongense</i> |
| 9 | 17. Pellis consisting of pseudoparenchyma |
| 8'. Peridium verrucose or leathery | 18 |
| 12 | 17'. Pellis consisting of interwoven cells |
| 9. Ascospore spines commonly curved or hooked | <i>T. crassitunicatum</i> |
| 10 | 18. Ascospore reticulate |
| 19 | 19 |
| 9'. Ascospore spines not commonly curved or hooked | 18'. Ascospore not reticulate |
| 11 | 24 |
| | 19. Ascospore alveolate-reticulate |
| | <i>T. microspiculatum</i> |
| | 19'. Ascospore spiny-reticulate or spiny |
| | 20 |
| | 20. Ascospore globose in shape |
| | 21 |
| | 20'. Ascospore ellipsoid in shape |
| | 22 |
| | 21. Peridium color yellow brown to dark brown; 130– |
| | 260 µm thick |
| | <i>T. lannaense</i> |
| | 21'. Peridium color yellow white; 200–250 µm thick |
| | <i>T. wanglangense</i> |
| | 22. Peridium thickness >300 µm |
| | <i>T. furfuraceum</i> |
| | 22'. Peridium thickness <300 µm |
| | 23 |
| | 23. Ascoma deeply and densely furrowed |
| | <i>T. taiyuanense</i> |

- 23'. Ascoma mostly smooth with few furrows
 *T. wenchuanense*
24. Ascospore globose in shape *T. lishanense*
- 24'. Ascospore ellipsoid in shape *T. piceatum*

ACKNOWLEDGMENTS

B.R. thanks Rachel Sanders, Michael Pezzetti, and Soroush Smith for laboratory assistance. B.R. is also grateful for the companionship and enthusiasm of Dakota Rennick, a German Shepherd truffle dog who located several of the *T. rugosum* truffles prior to his premature death.



DISCLOSURE STATEMENT

No potential conflict of interest was reported by the author(s).

FUNDING

G.B. acknowledges Michigan State University (MSU) AgBioResearch National Institute of Food and Agriculture NIFA project MICL02416 and National Science Foundation (NSF) grant 1946445. G.B. and B.R. acknowledge support from Project GREEN (GR18-076) and the MSU Plant, Soil and Microbial Sciences Endowed Graduate Assistantship to B. R. R.H. thanks St. John's University for permission to collect on their campus, the Minnesota Department of Natural Resources for funding and permission to collect (Special Permit No. 2009-42) at Nerstrand Big Woods State Park, and the Society of Systematics Biologists for funding for sequencing work.

ORCID

B. Rennick  <http://orcid.org/0000-0002-0742-2279>
 G. M. N. Benucci  <http://orcid.org/0000-0003-1589-947X>
 Zhi-Yan Du  <http://orcid.org/0000-0001-7646-2429>
 R. Healy  <http://orcid.org/0000-0001-7616-0092>
 G. Bonito  <http://orcid.org/0000-0002-7262-8978>

LITERATURE CITED

- Adobe Inc. 2019a. Adobe Illustrator (23.0.3) [software]. Adobe Inc. [accessed 2021 Nov 16]. <https://adobe.com/products/illustrator.html>
- Adobe Inc. 2019b. Adobe photoshop (23.0.1) [software]. Adobe Inc. [accessed 2021 Dec 14]. <https://www.adobe.com/products/photoshop.html>
- Angelini P, Tirillini B, Fiorini D, Bricchi E, Venanzoni R. 2015. Can the fatty acids profile of *Tuber aestivum* – *T. uncinatum* species complex have chemotaxonomic value? *Flora Mediterranea*. 25:10.
- Beyer WN, Saari DM. 1978. Activity and ecological distribution of the slug, *Arion subfuscus* (Draparnaud) (Stylommatophora, Arionidae). *The American Midland Naturalist*. 100(2):359–367. doi:10.2307/2424835.
- Bonito G, Smith ME, Nowak M, Healy RA, Guevara G, Cazares E, Kinoshita A, Nouhra ER, Dominguez LS, Tedersoo L, et al. 2013. Historical biogeography and diversification of truffles in the Tuberales and their newly identified southern hemisphere sister lineage. *PLoS One*. 8(1):e52765–e52765. doi:10.1371/journal.pone.0052765.
- Bonito GM, Gryganskyi AP, Trappe JM, Vilgalys R. 2010. A global meta-analysis of *Tuber* ITS rDNA sequences: species diversity, host associations and long-distance dispersal. *Molecular Ecology*. 19(22):4994–5008. doi:10.1111/j.1365-294X.2010.04855.x.
- Bouatia M, Touré H, Cheikh A, Eljaoudi R, Rahali Y, Idrissi MOB, Khabar L, Draoui M. 2018. Analysis of nutrient and antinutrient content of the truffle (*Tirmania pinoyi*) from Morocco. *International Food Research Journal*. 25:174–178.
- Butters FK. 1903. A Minnesota species of *Tuber*. *Botanical Gazette*. 35(6):427–31. doi:10.1086/328364.
- Buzzini P, Gasparetti C, Turchetti B, Cramarossa MR, Vaughan-Martini A, Martini A, Pagnoni UM, Forti L. 2005. Production of volatile organic compounds (VOCs) by yeasts isolated from the ascocarps of black (*Tuber melanosporum* Vitt.) and white (*Tuber magnatum* Pico) truffles. *Archives of Microbiology*. 184(3):187–193. doi:10.1007/s00203-005-0043-y.
- Cao JZ, Chi WD, Fan L, Li Y. 2011. Notes on the neotype of *Tuber taiyuanense*. *Mycotaxon*. 116(1):7–11. doi:10.5248/116.7.
- Cázares E, Trappe JM. 1994. Spore dispersal of ectomycorrhizal fungi on a glacier forefront by mammal mycophagy. *Mycologia*. 86(4):507–510. doi:10.2307/3760743.
- Chen J, Liu PG, Wang Y. 2005. *Tuber umbilicatum*, a new species from China, with a key to the spinose-reticulate spored *Tuber* species. *Mycotaxon*. 94: 1–6.
- Deng XJ, Chen J, Yu FQ, Liu PG. 2009. Notes on *Tuber huidongense* (Tuberales, Ascomycota), an endemic species from China. *Mycotaxon*. 109(1):189–199. doi:10.5248/109.189.
- Eberhart J, Trappe J, Páez CP, Bonito G. 2020. *Tuber luomae*, a new spiny-spored truffle species from the Pacific Northwest, USA. *Fungal Systematics and Evolution*. 6(1):299–304. doi:10.3114/fuse.2020.06.15.
- Edgar RC. 2004. MUSCLE: a multiple sequence alignment method with reduced time and space complexity. *BMC Bioinformatics*. 5(1):113. doi:10.1186/1471-2105-5-113.
- Elliott T, Türkoğlu A, Trappe J, Yaratankul Güngör M. 2016. Turkish truffles 2: eight new records from Anatolia. *Mycotaxon*. 131(2):439–453. doi:10.5248/131.439.
- Enrico L, Paolo F, Mirco I, Antonio F, Alessandra Z. 2016. *Tuber melosporum* smooth spores: an anomalous feature in the genus *Tuber*. *Mycologia*. 108(1):174–178. doi:10.3852/15-080.
- Eslick H. 2012. Identifying the cause of rot in black truffles and management control options. Australia: Rural Industries Research and Development Corporation. p. 46.
- Fan L, Cao JZ, Hou CL. 2013. *Tuber subglobosum* and *T. wenchuanense* - two new species with spino-reticulate ascospores. *Mycotaxon*. 123(1):95–101. doi:10.5248/123.95.
- Fan L, Cao JZ, Zheng ZH, Li Y. 2012. *Tuber* in China: *T. microspermum* and *T. microspiculatum* spp. nov. *Mycotaxon*. 119(1):391–395. doi:10.5248/119.391.
- FigTree. 2018. Ver. 1.4.4. [software]. <http://tree.bio.ed.ac.uk/software/figtree/>
- Frank J, Southworth D, and Trappe J. 2006. NATS truffle and truffle-like fungi 13: *Tuber quercicola* and *T. whetstonense*,

- new species from Oregon, and *T. candidum* redescribed. *Mycotaxon*. 95:229–240.
- Gabel A, Ackerman C, Gabel M, Krueger E, Weins S, Zierer L. 2010. Diet and habitat of northern flying squirrels (*Glaucomys sabrinus*) in the Black Hills of South Dakota. *Western North American Naturalist*. 70(1):92–104. doi:10.3398/064.070.0110.
- Gardes M, Bruns TD. 1993. ITS primers with enhanced specificity for basidiomycetes—application to the identification of mycorrhizae and rusts. *Mol Ecol*. 2(2). doi:10.1111/j.1365-294x.1993.tb00005.x.
- Geyer CJ. 1991. *Markov Chain Monte Carlo Maximum Likelihood*. [accessed 2021 Mar 3]. <http://conservancy.umn.edu/handle/11299/58440>
- Gimeno A, Leimgruber M, Kägi A, Jenny E, Vogelgsang S. 2021. UV protection and shelf life of the biological control agent *Clonostachys rosea* against *Fusarium graminearum*. *Biological Control*. 158:104600.
- Granetti B, Mincigrucci G, Bricchi E. 1988. Analisi biometrica e morfologica delle ascospore di alcune specie del genere *Tuber*. *ATTI 2° Congresso Internazionale Sul Tartufo Di Spoleto - 1988*. 59–100.
- Grunow A, Rabenhorst L. 1884. Dr. L. Rabenhorst's kryptogamen-flora von Deutschland, Oesterreich und der Schweiz. Leipzig, Germany: E. Kummer.
- Harkness HW 1899. Californian Hypogaeous fungi. *Proceedings of the California Academy of Sciences*. San Francisco, CA, USA. [accessed 2021 Dec 8]. <https://www.biodiversitylibrary.org/page/13793910#page/77/mode/1up>
- Healy R, Bonito GM, Smith ME. 2016. A brief overview of the systematics, taxonomy, and ecology of the *Tuber rufum* clade. In: Zambonelli A, Iotti M, Murat C editors. *True Truffle (Tuber spp.) in the world*. *Soil biology*. Vol. 47. Cham: Springer. p. 125–136. https://doi.org/10.1007/978-3-319-31436-5_8
- Hochberg M, Bertault G, Poitrineau K, Janssen A. 2003. Olfactory orientation of the truffle beetle, *Leiodes cinnamomea*. *Entomologia Experimentalis et Applicata*. 109(2):147–153. doi:10.1046/j.1570-7458.2003.00099.x.
- Hu HT, Wang Y. 2005. *Tuber furfuraceum* sp. Nov. From Taiwan. *Mycotaxon*. 93:155–157.
- Huelsenbeck JP, Ronquist F. 2001. MRBAYES: bayesian inference of phylogenetic trees. *Bioinformatics*. 17(8):754–755. doi:10.1093/bioinformatics/17.8.754.
- Kitabayashi K, Tuno N. 2018. Soil burrowing *Muscina angustifrons* (Diptera: Muscidae) larvae excrete spores capable of forming mycorrhizae underground. *Mycoscience*. 59(3):252–258. doi:10.1016/j.myc.2018.02.003.
- Lancellotti E, Iotti M, Zambonelli A, Franceschini A. 2016. The puberulum group sensu lato (Whitish Truffles). In: Zambonelli A, Iotti M, Murat C, editors. *True Truffle (Tuber spp.) in the World: Soil Ecology, Systematics and Biochemistry*. Springer International Publishing. p. 105–124. doi:10.1007/978-3-319-31436-5_7.
- Leonardi M, Ascione S, Pacioni G, Cesare P, Pacioni ML, Miranda M, Zarivi O. 2018. The challenge for identifying the fungi living inside mushrooms: the case of truffle inhabiting mycelia. *Plant Biosystems*. 152(5):1002–1010. doi:10.1080/11263504.2017.1407373.
- Leonardi M, Paz-Conde A, Guevara G, Salvi D, Pacioni G. 2019. Two new species of *Tuber* previously reported as *Tuber malacodermum*. *Mycologia*. 111(4):676–689. doi:10.1080/00275514.2019.1603777.
- Liber JA, Minier DH, Stouffer-Hopkins A, Van Wyk J, Longley R, Bonito G. 2022. Maple and hickory leaf litter fungal communities reflect pre-senescent leaf communities. *PeerJ*. 10:e12701.
- Maddison WP, Maddison DR. 2019. *Mesquite: a modular system for evolutionary analysis* Ver. 3.61. [software]. [accessed 2021 Nov 16]. <http://www.mesquiteproject.org>
- Martin F, Kohler A, Murat C, Balestrini R, Coutinho PM, Jaillon O, Montanini B, Morin E, Noel B, Percudani R, et al. 2010. Périgord black truffle genome uncovers evolutionary origins and mechanisms of symbiosis. *Nature*. 464(7291):1033–1038. doi:10.1038/nature08867.
- Maser C, Claridge A, Trappe J, Krebs C. 2008. *Trees, truffles, and beasts: how forests function*. Rutgers University Press. [accessed 2021 Nov 16]. <https://muse.jhu.edu/book/15663>
- McGraw R, Duncan N, Cazares E. 2002. Fungi and other items consumed by the blue-gray taildropper slug (*Prophyaon coeruleum*) and the papillose taildropper slug (*Prophyaon dubium*). *The Veliger*. 45:261–264.
- Miller MA, Pfeiffer W, Schwartz T 2010. Creating the CIPRES Science Gateway for inference of large phylogenetic trees. 2010 Gateway Computing Environments Workshop (GCE). New Orleans, LA, USA. p. 1–8. <https://doi.org/10.1109/GCE.2010.5676129>
- Ori, et al. 2021. Effect of slug mycophagy on *Tuber aestivum* spores. *Fungal Biology*. 125(10):796–805. doi:10.1016/j.funbio.2021.05.002
- Ori F, Trappe J, Leonardi M, Iotti M, Pacioni G. 2018. Crested porcupines (*Hystrix cristata*): mycophagist spore dispersers of the ectomycorrhizal truffle *Tuber aestivum*. *Mycorrhiza*. 28(5-6):561–565. doi:10.1007/s00572-018-0840-1.
- Pacioni G, Leonardi M, Aimola P, Ragnelli AM, Rubini A, Paolucci F. 2007. Isolation and characterization of some mycelia inhabiting *Tuber* ascomata. *Mycological Research*. 111(12):1450–1460. doi:10.1016/j.mycres.2007.08.016.
- Pavic A, Stanković S, Saljnikov E, Krüger D, Buscot F, Tarkka M, Marjanović Ž. 2013. Actinobacteria may influence white truffle (*Tuber magnatum* Pico) nutrition, ascocarp degradation and interactions with other soil fungi. *Fungal Ecology*. 6(6):527–538. doi:10.1016/j.funeco.2013.05.006.
- Pelusio F, Nilsson T, Montanarella L, Tilio R, Larsen B, Facchetti S, Madsen J. 1995. Headspace solid-phase microextraction analysis of volatile organic sulfur compounds in black and white truffle aroma. *Journal of Agricultural and Food Chemistry*. 43(8):2138–2143. doi:10.1021/jf00056a034.
- Piattoni F, Oir F, Morara M, Iotti M, Zambonelli A. 2013. The role of wild boars in spore dispersal of hypogeous fungi. *Acta Mycologica; Polish Botanical Society*. 47(2):145–153. doi:10.5586/am.2012.017.
- Puliga F, Illice M, Iotti M, Baldo D, Zambonelli A. 2020. *Tuber iranicum*, sp. nov., a truffle species belonging to the excavatum clade. *Mycologia*. 112(5). doi:10.1080/00275514.2020.1783181.
- Rambaut A, Drummond AJ, Xie D, Baele G, Suchard MA. 2018. Posterior summarization in Bayesian phylogenetics using Tracer 1.7. *Systematic Biology*. 67(5):901–904. doi:10.1093/sysbio/syy032.

- Rivera CS, Blanco D, Oria R, Venturini ME. 2010. Diversity of culturable microorganisms and occurrence of *Listeria monocytogenes* and *Salmonella* spp. In *Tuber aestivum* and *Tuber melanosporum* ascocarps. Food Microbiology. 27(2):286–293. doi:10.1016/j.fm.2009.11.001.
- Ronquist F, Huelsenbeck JP. 2003. MrBayes 3: bayesian phylogenetic inference under mixed models. Bioinformatics. 19(12):1572–1574. doi:10.1093/bioinformatics/btg180.
- Shah NN, Hokkanen S, Pastinen O, Eljamil A, Shamekh S. 2020. A study on the fatty acid composition of lipids in truffles selected from Europe and Africa. 3 Biotech. 10(10):415. doi:10.1007/s13205-020-02414-y.
- Splivallo R, Ottonello S, Mello A, Karlovsky P. 2011. Truffle volatiles: from chemical ecology to aroma biosynthesis. New Phytologist. 189(3):688–699. doi:10.1111/j.1469-8137.2010.03523.x.
- Spurr AR. 1969. A low-viscosity epoxy resin embedding medium for electron microscopy. Journal of Ultrastructure Research. 26(1):31–43. doi:10.1016/S0022-5320(69).
- Stamatakis A. 2014. RAxML version 8: a tool for phylogenetic analysis and post-analysis of large phylogenies. Bioinformatics. 30(9):1312–1313. doi:10.1093/bioinformatics/btu033.
- Suwannarach N, Kumla J, Vadthananat S, Raspé O, Lumyong S. 2016. Morphological and molecular evidence support a new truffle, *Tuber lannaense*, from Thailand. Mycological Progress. 15(8):827–834. doi:10.1007/s11557-016-1212-x.
- Trappe J, Jumpponen A, Cazares E. 1996. Nats truffle and truffle-like fungi 5: *Tuber Iyonii* (= *T. texense*), with a key to the spiny-spored *Tuber* species groups. Mycotaxon. 60:365–372.
- Uecker FA, Burdsall HH. 1977. *Tuber spinoreticulatum*, a new truffle from Maryland. Mycologia. 69(3):626–630. doi:10.1080/00275514.1977.12020102.
- Vilgalys R, Hester M. 1990. Rapid genetic identification and mapping of enzymatically amplified ribosomal DNA from several cryptococcus species. Journal of Bacteriology. 172(8). doi:10.1128/jb.172.8.4238-4246.1990.
- Vittadini C. 1831. Monographia Tubercarum. ex typographia F. Rusconi, Milan. [accessed 2021 Dec 8]. <http://archive.org/details/monographiatube00vittgoog>
- Wang S, Marcone MF. 2011. The biochemistry and biological properties of the world's most expensive underground edible mushroom: truffles. Food Research International. 44(9):2567–2581. doi:10.1016/j.foodres.2011.06.008.
- Wang Y. 1988. First report of a study on *Tuber* species from China. ATTI 2° Congresso Internazionale Sul Tartufo Di Spoleto – 1988. 45–50.
- Yan X, Cao J, Fan L. 2018. Four new *Tuber* species added to the Rufum group from China based on morphological and molecular evidence. Mycologia. 110(4):771–779. doi:10.1080/00275514.2018.1490120.
- Yan X, Wang Y, Sang X, Fan L. 2017. Nutritional value, chemical composition and antioxidant activity of three *Tuber* species from China. AMB Express. 7(1). doi:10.1186/s13568-017-0431-0.